LOCAL FREQUENCY ANALYSIS OF CHAOTIC MOTION IN MULTIDIMENSIONAL SYSTEMS: ENERGY TRANSPORT AND BOTTLENECKS IN PLANAR OCS

Craig C. MARTENS [a,1,2], Michael J. DAVIS [b] and Gregory S. EZRA [a,3]
[a] Department of Chemistry, Baker Laboratory, Cornell University, Ithaca, NY 14853, USA
[b] Chemistry Division, Argonne National Laboratory, Argonne, IL 60439, USA

Received 25 September 1987

The method of local frequency analysis for study of chaotic motion in multidimensional systems is described, and applied to the analysis of intramolecular energy flow in a three-mode model for OCS. The nature of possible partial barriers responsible for long-time correlations in multimode systems is discussed.

1. Introduction

Recent research on classical theories of unimolecular and bimolecular processes in two-mode systems has established the important role of dynamical bottlenecks in non-statistical behavior [1-5]. Previous work on long-time correlations in area preserving maps has identified two types of partial barrier to transport in chaotic regions of phase space [6-8]. The first are invariant Cantor sets, called cantori [6], which are remnants of invariant tori that have broken up under the influence of non-integrable perturbations. The second are broken separatrices [8], which form the boundaries of resonance zones [9], or, in the case of dissociative dynamics, the remnants of the last bound phase curves [2]. Transport across both cantori and broken separatrices [9,10] has been incorporated into statistical models of intramolecular vibrational energy relaxation (IVR) [1], vibrational predissociation of van der Waals molecules [2], isomerization [3] and bimolecular reaction rates [4,5] in two-degree of freedom (DOF) systems.

The phase space structures associated with trapping and long-time correlations in two DOF are most naturally characterized in terms of relations between the frequencies of motion. The least permeable cantori, which form minimum flux intramolecular transition states for IVR, are the remnants of invariant tori with the most irrational frequency ratios [6]. Physically, these robust tori are those for which the two coupled modes are farthest from resonance [11]. Trapping of trajectories inside a resonance zone is associated with a locking of the two fundamental frequencies into a particular rational ratio [12].

The nature of the bottlenecks responsible for trapping in $N\geqslant 3$-mode systems [13,14] is at present unknown. The structure of chaotic phase space for $N\geqslant 3$ DOF is qualitatively different from the two-mode case, due mainly to the fact that invariant N-tori cannot partition the $(2N-1)$-dimensional energy surface for $N>2$, and relaxation pathways and mechanisms for long-time correlations are poorly understood. The studies that have led to the present understanding of the two-mode case have relied on techniques, such as the Poincare surface of section [11], which are not readily applicable to higher-dimensional systems. Since real polyatomics have at least three vibrational modes, an understanding of phase space structure in higher dimensions is clearly desirable.

[1] Mathematical Sciences Institute Fellow.
[2] Present address: Department of Chemistry, University of Pennsylvania, Philadelphia, PA 19104, USA.
[3] Alfred P. Sloan Fellow.

0 009-2614/87/$ 03.50 © Elsevier Science Publishers B.V.
(North-Holland Physics Publishing Division)

The present note summarizes our recent work on the intramolecular dynamics of polyatomic molecules, with a particular focus on the distinctive features of multidimensional transport exhibited by a three-DOF model for OCS constrained to vibrate in a space-fixed plane ("planar OCS") [13,14]. We first describe a new methodology for studying chaotic dynamics in multimode systems, based upon local frequency analysis of non-quasiperiodic trajectories. The structure of phase space for three-DOF systems is then briefly considered, with particular attention given to the importance of relations between the local frequencies. Application of local frequency analysis to planar OCS is discussed, and the resulting picture of transport and trapping summarized. A detailed account will be given elsewhere [15]. We note that parallel work on the phase space structure of three-DOF systems has been done by Gillilan and Reinhardt [16].

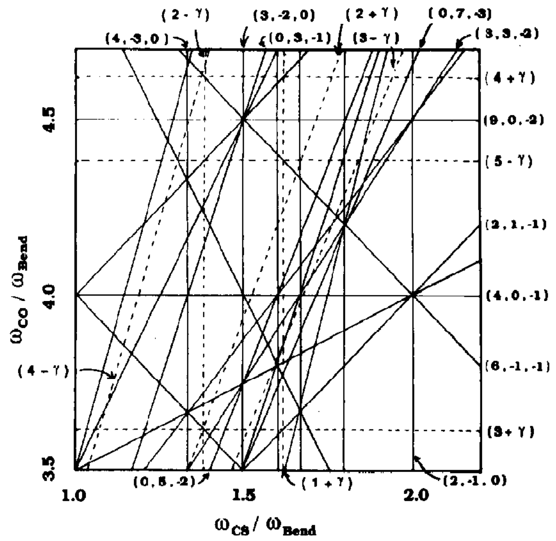

Fig. 1. Frequency ratio space for planar OCS. Resonance lines (solid) and pairwise noble conditions (dashed) are indicated.

2. Local frequency analysis and dynamics in frequency ratio space

To motivate our approach to the analysis of chaotic dynamics in multimode systems, consider bound motion described by an integrable Hamiltonian $H^0(I)$ [11], where $\{I\}$ is a set of zeroth-order action variables, $\omega(I) = \partial H^0(I)/\partial I$ are the corresponding frequencies, and H^0 is taken to approximate the Hamiltonian H of interest. If the relation between the actions and frequencies is invertible, the frequencies themselves can be used in place of the actions as phase space coordinates. In a three-mode system, the energy shell can be projected onto a 2D space of two independent frequency ratios (winding numbers); the resulting "tune space" [17] is shown in fig. 1 for planar OCS, and is a key element in our understanding of three-DOF transport.

Whereas the actions $\{I\}$, and hence the frequencies $\omega(I)$, are constant under the motion generated by H^0, they are time dependent for non-quasiperiodic trajectories of the full Hamiltonian H [11]. By defining *local frequencies* of the motion (see below), the time evolution of non-quasiperiodic trajectories can be followed in frequency ratio space. Just as for two-DOF systems, important phase space structures in three-DOF (those leading to either enhanced transport or trapping) can be defined by relations between frequencies of motion. A local frequency analysis of the motion therefore focuses attention directly on the aspect of central importance for dynamics.

The utility of local frequency analysis for chaotic trajectories of 3D OCS is based on the empirical observation that, although the motion may be manifestly irregular [11] when viewed over long-time scales (≈ 50 ps), quantities such as fundamental frequencies and short-time averages of zeroth-order actions and mode energies are often fairly constant over times (≈ 1 ps) corresponding to many vibrational periods. Trajectories are localized in particular regions of phase space characterized by these properties. Although non-quasiperiodic trajectories will eventually pass from one such region to another, the existence of long-time correlations implies that the mean lifetime in a region is typically considerably longer than either a vibrational period or the local relaxation rate implied by, say, the maximal Lyapunov exponent [18,19] (conversely, this may be taken as an operational definition of a dynamically significant region of phase space).

Local frequency analysis of chaotic motion is accomplished by performing fast Fourier transforms of short (1.4 ps) sequential segments of trajectories. The procedure used is described in detail elsewhere [15].

The different regions occupied by a trajectory are characterized by the local frequencies, or by their ratios (coordinates in frequency ratio space), and the evolution of the system can be studied by following the changes of the local frequencies with time. The trajectory segments used to define local frequencies must be long enough to allow sufficient frequency resolution, but short enough to ensure that the dynamical correlations of interest occur on a time scale longer than the segment length. This calculation [15] yields time-dependent "local frequencies" for chaotic trajectories.

Local frequency analysis is a useful method for the study of chaotic dynamics in multimode systems. For example, it is straightforward to determine whether a trajectory segment satisfies one or more resonance conditions of the form $\boldsymbol{k}\cdot\boldsymbol{\omega}=0$, or whether a particular local frequency ratio passes through a given value. By simply counting the number of times a given condition on the local frequencies is satisfied along a given trajectory, it is possible to calculate fluxes across dividing surfaces defined in terms of the frequencies without having to construct the surface itself [15]. It is thereby possible to investigate the nature of dynamical bottlenecks in multidimensional phase space.

The calculation of Fourier spectra of short segments of long trajectories has been previously discussed by McDonald and Marcus [20] and Marcus, Hase, and Swamy [21]. Their emphasis, however, was on the time dependence of Fourier *amplitudes* as an indicator of the dynamics; they did not analyze the local frequencies.

3. Phase space structure for three degrees of freedom

To help interpret our trajectory results for planar OCS, it is useful to briefly survey the structure of phase space for three DOF, with reference to the frequency ratio space of fig. 1. A detailed account is given elsewhere [15].

The portion of frequency ratio space corresponding to the dynamically accessible region of planar OCS is shown in fig. 1. Coordinates are the ratios $\omega_{\mathrm{CS}}/\omega_{\mathrm{bend}}$ (x axis), ranging from 1.0 to 2.2, and $\omega_{\mathrm{CO}}/\omega_{\mathrm{bend}}$ (y axis), ranging from 3.5 to 4.7. For an integrable three-DOF Hamiltonian $H^0(\boldsymbol{I})$, each point in frequency ratio space represents an invariant torus, specified uniquely by two frequency ratios and the energy (equivalent to specifying the three actions $\boldsymbol{I}$).

The solid straight lines in frequency ratio space identify multidimensional *resonance zones*; that is, families of frequencies satisfying a single resonance condition of the form

$$\boldsymbol{k}\cdot\boldsymbol{\omega}=0\,, \tag{1}$$

with $\boldsymbol{k}=(k_{\mathrm{bend}}, k_{\mathrm{CS}}, k_{\mathrm{CO}})$ a vector of integers. For example, vertical solid lines correspond to the pairwise frequency locking $\omega_{\mathrm{CO}}/\omega_{\mathrm{bend}}=$constant, while sloping solid lines passing through the origin of frequency ratio space correspond to $\omega_{\mathrm{CO}}/\omega_{\mathrm{CS}}=$rational. Sloping solid lines that do not pass through the origin correspond to a general ("ternary") resonance condition with all components of the vector $\boldsymbol{k}$ nonzero. For H^0, the resonance condition defines a one-parameter family of resonant tori. For a non-integrable Hamiltonian H, condition (1) defines a resonance zone, a 5D region of phase space with associated stochastic layer and multidimensional broken separatrix (a 4D surface). An important aspect of dynamics in $N\geqslant3$-DOF systems is the possibility of transport *along* resonance zones [11], that is, along the solid lines in fig. 1 (see section 4).

The dense network of resonance lines in the frequency ratio plane forms the Arnold web [11]. Only a few of the lowest-order resonances important in planar OCS are shown in fig. 1. At the intersection of every pair of resonance lines two independent resonance conditions are satisfied, $\boldsymbol{k}\cdot\boldsymbol{\omega}=0$ and $\boldsymbol{k}'\cdot\boldsymbol{\omega}=0$, say, implying an infinity of resonance conditions $n\boldsymbol{k}\cdot\boldsymbol{\omega}+n'\boldsymbol{k}'\cdot\boldsymbol{\omega}=0$ (n, n' integer). For H^0, the intersection of two resonance lines specifies a single torus consisting of a two-parameter family of periodic orbits. For a non-integrable Hamiltonian H, the junction of two resonance zones is a dynamically significant region of phase space. Trajectories can "turn the corner" from one resonance zone to another at the resonance junctions, and the cumulative effect of the resulting changes in direction is a diffusive wandering, known as Arnold diffusion [11,12]. Extensive trapping of trajectories in the vicinity of resonance junctions is found in planar OCS (see section 4); this effect appears to have received little previous attention.

We now consider the nature of possible bottlenecks to IVR in three DOF. Single tori or cantori, which define 3D invariant or near invariant manifolds, cannot act as barriers on the 5D energy shell. However, a single constraint on the frequencies, $F(\omega)=0$, defines a 4D surface in phase space (in the integrable case, a one-parameter family of tori). Such a surface has the correct dimension to divide the 5D energy shell into disjoint regions. In addition, the 4D broken separatrices associated with three-DOF resonance zones have the right dimensionality to act as partial barriers to transport in and out of resonance zones.

Which conditions $F(\omega)$ define dynamical bottlenecks in three-DOF systems? Is it possible to find single constraints that define bottlenecks globally, or are partial barriers best defined piecewise by a set of local constraints on the frequencies? Definitive answers to these central questions cannot be given as yet. The notion that partial barriers to transport are associated with sets of particularly robust tori suggests, however, that any such constraints should reflect extreme mutual irrationality of the frequencies. Local frequency analysis is therefore a most effective way of identifying such bottlenecks in multimode systems.

An example of a global constraint is the *pairwise irrationality* condition

$$\omega_i/\omega_j=\text{Noble}\,. \qquad (2)$$

(Noble numbers are highly irrational numbers of the form $(n+n'\gamma)/(m+m'\gamma)$, with $\gamma=\frac{1}{2}(5^{1/2}-1)$, the golden mean, and $nm'-n'm=\pm1$ [6].) Eq. (2) is the simplest possible generalization from the well studied two-mode case to three-DOF systems. For an integrable problem, condition (2) defines a one-parameter family of invariant tori. Under a non-integrable perturbation, this 4D manifold develops an infinity of "resonant holes", corresponding to simultaneous satisfaction of conditions (1) and (2). The existence of the resonant holes means that, even for arbitrarily small couplings, condition (2) does not define an absolute barrier to transport. Nonetheless, since most resonances are high order and/or not strongly driven by coupling terms in the Hamiltonian, it is conceivable that noble pairwise bottlenecks defined by (2) may impede transport in certain regions of phase space, i.e. lead to long-time correlations in $N\geqslant3$-DOF systems. This possibility is consistent with trajectory data on OCS discussed below. In the limit that all modes but i and j uncouple, the pairwise irrationality condition (2) defines a cantorus in the two-DOF i,j subspace; this limiting behavior suggests that the 4D bottlenecks defined by (2) may act as barriers to transport in regions of phase space close to the relevant two-DOF subspace.

Pairwise irrational surfaces are represented by straight dashed lines in fig. 1. For example, the sloping dashed line corresponding to the irrational frequency ratio $\omega_{CO}/\omega_{CS}=2+\gamma$ falls between the solid lines associated with the resonance vectors $(0,3,-1)$ and $(0,5,-2)$.

Pairwise irrationality conditions are certainly not the only candidates for three-DOF bottlenecks. Some other more general possibilities are discussed in section 4.

4. Energy relaxation and long-time correlations in planar OCS

We now illustrate the general considerations of section 3 by examining representative trajectories for 3D OCS at a single energy, $E=20000$ cm^{-1} ($\approx90\%$ of the dissociation energy). At this energy, most trajectories are quite chaotic, as indicated by their nonzero Lyapunov exponents [13,14]. The trajectories shown below have been selected from 8 ensembles of 50 trajectories each (400 total). Each trajectory is 45 ps long, and is divided into 128 overlapping segments, as described above. Careful analysis of all 400 trajectories was performed, and it was found that several distinct patterns of dynamical behavior appeared repeatedly in the data. These patterns are now illustrated with some typical trajectories.

4.1. Transport along resonance zones

Fig. 2a shows time-dependent local frequency ratios and segment-averaged mode energies for a typical chaotic trajectory of planar OCS. The top frame gives the CS/bend frequency ratio, the second frame shows the CO/CS ratio, while the third frame gives the CO/bend value. For certain segments, more than

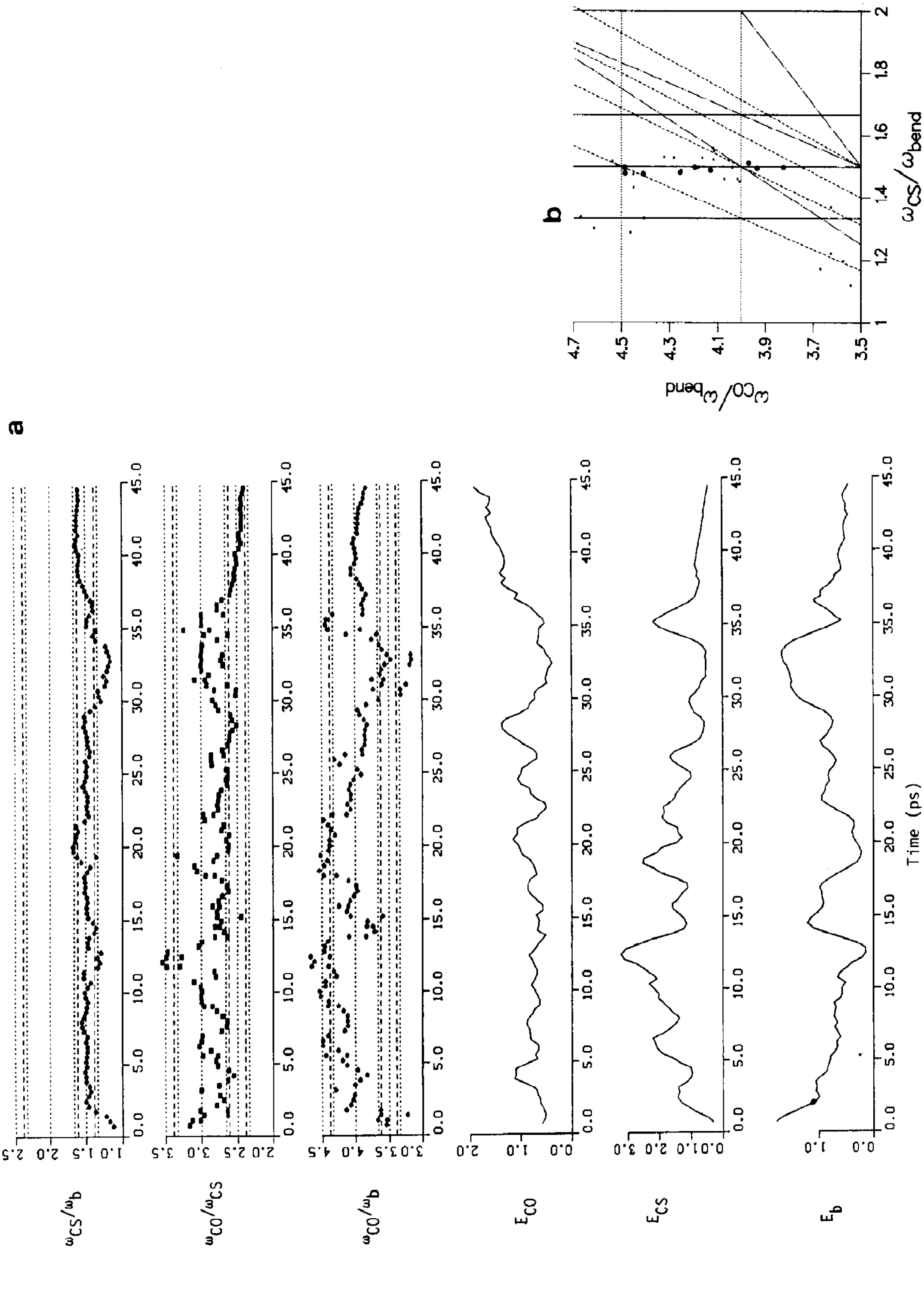

Fig. 2. (a) Local frequency ratios and locally averaged mode energies versus time for a chaotic trajectory of planar OCS. From the top: CS/bend, CO/CS and CO/bend frequency ratios, locally averaged CO normal, CS normal and bend normal mode energies. This trajectory shows transport along the CS/bend 3 : 2 resonance zone. (b) Time development of the local frequency ratios for the first 12.8 ps (36 segments) of the trajectory of (a). Segments 10–19 are shown with large dots; this portion of the trajectory stays along the 3 : 2 resonance line for 3.1 ps.

one local frequency ratio is plotted; these are ambiguous segments, having spectra with at least two peaks of comparable intensity. Also included are horizontal lines, indicating pairwise resonant conditions (dotted) and noble ratios $M \pm \gamma$, M integer (dashed). The bottom three frames show segment-averaged normal mode energies for CO stretch, CS stretch, and bend, respectively.

The local frequency ratios change with time, sometimes smoothly and continuously, sometimes sharply and discontinuously. Changes in the frequency ratios can be correlated with the normal mode energy exchange by noting that, whereas the CO and CS mode frequencies decrease with increasing excitation, the bend frequency *increases* when energy is transferred into bending motion.

A notable feature of the trajectory of fig. 2a is the occurrence of several groups of segments (for example, from 3.9 to 7 ps) where the CS/bend frequency ratio is fairly constant around the value 1.5. While $\omega_{CS}/\omega_{bend}$ executes small fluctuations about this value, the other frequency ratios, and the normal mode energies, show substantial changes. Configuration space projections [15] clearly show the trajectory entering a region of phase space characterized by a 3 : 2 resonance between the CS and bend modes. Between 3.9 and 7 ps, large changes in local frequencies and mode energies occur, indicating exchange of energy between the modes. Nevertheless, *the CS and bend modes remain locked in a 3 : 2 resonance throughout these changes.* When plotted in frequency ratio space, the trajectory points move up and down along the vertical line corresponding to the resonance vector $(3, -2, 0)$ (fig. 2b).

The picture that emerges from application of local frequency analysis to this and other similar examples is one of the CS/bend 3 : 2 resonance zone acting as a pathway for facile energy exchange in planar OCS. Transport along the $(0, 4, -1)$ resonance zone is also found to be important in 3D OCS.

4.2. Long-time correlations near junctions of resonance zones

We consider now another type of behavior seen in planar OCS. Fig. 3 shows a trajectory for which the motion is localized for about 20 ps before any significant energy exchange occurs. During this time, the local frequency ratios change by a series of small steps. Detailed examination of the frequency data shows that the trajectory gets trapped for several segments in the vicinity of a resonance junction, then rapidly jumps to another, where it remains for several more segments, and so on. Many other examples of localization at resonance junctions can be found in the full trajectory ensemble [15].

4.3. Dynamical barriers to chaotic transport

At about 20 ps, the trajectory shown in fig. 3 begins a period of more active energy exchange. The abrupt change in behavior occurs when the CO/CS frequency ratio suddenly passes through the value $2+\gamma$. Just at the crossing point, the CO/bend frequency ratio satisfies a 4 : 1 resonance condition.

This behavior may be interpreted as follows: Locally, the $2+\gamma$ CO/CS surface acts as a dynamical bottleneck in three-DOF OCS. (Globally, however, the $2+\gamma$ surface may be only part of a larger dividing surface.) The trajectory wanders through a region of resonance junctions localized on one side of the barrier, until it enters the 4 : 1 CO/bend resonance zone, whereupon it rapidly passes through to a more chaotic region of phase space. The local division of phase space into two parts by a $2+\gamma$ pairwise bottleneck, one more chaotic than the other, is consistent with the well studied behavior of the limiting collinear configuration [1].

The above discussion is based on a "pairwise" view of the dynamics, in which partial barriers in three-DOF transport are assumed to consist of families of the corresponding two-DOF dividing surfaces. While this picture is appealing as a minimal extrapolation from the two-DOF problem, it cannot be valid in general, and new ideas must be developed to fully understand three-DOF dynamics. We now outline two new approaches to the problem of defining bottlenecks in three DOF, each based upon a generalization of number theoretic ideas that have been successful in understanding two-DOF systems.

The first approach focuses on the most robust *tori*. Kim and Ostlund have introduced an algorithm for generating simultaneously irrational *pairs* of irrational numbers [23]. They argue that these are the appropriate generalizations of the notion of noble frequency ratios to three DOF, so that the resulting

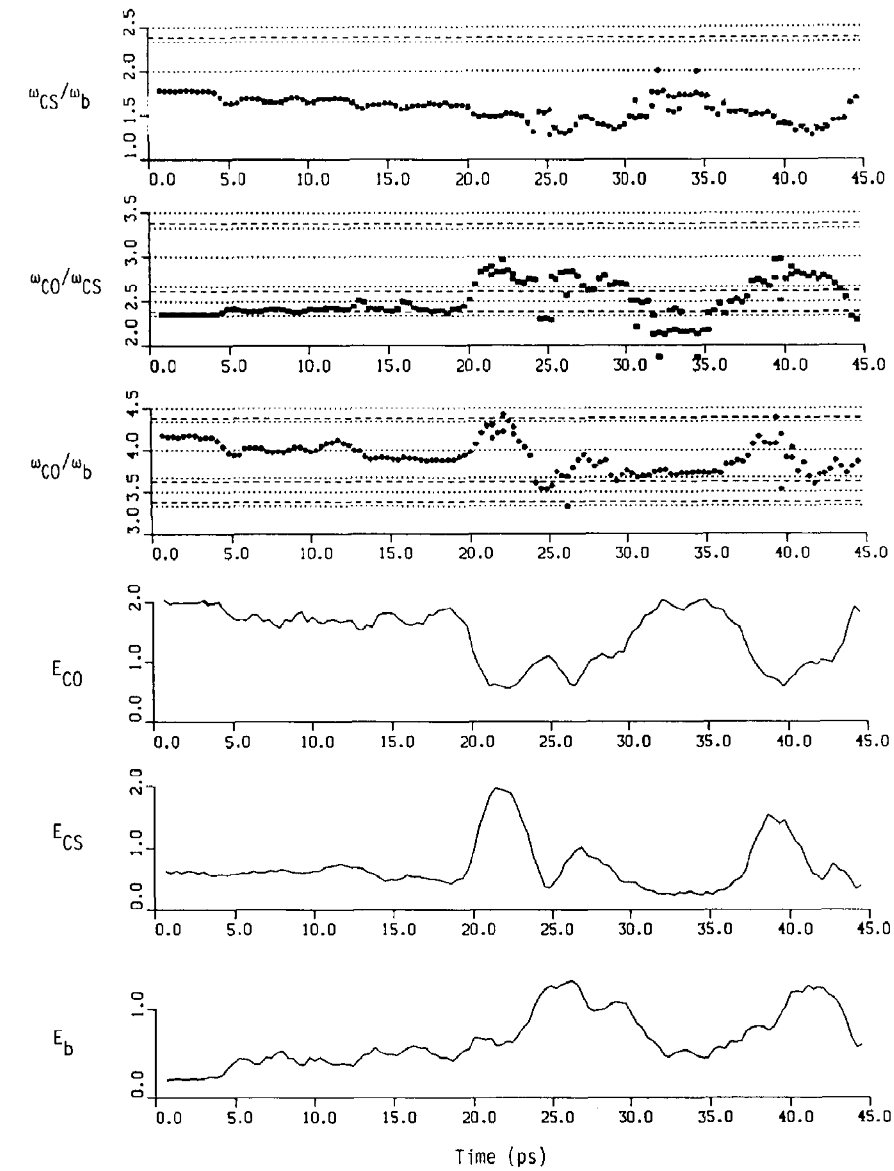

Fig. 3. Local frequency ratios and locally averaged mode energies versus time for a trajectory of planar OCS. This trajectory exhibits long-time trapping prior to a sudden transition to a more chaotic region of phase space. See caption of fig. 2a for details.

"spiral noble" pairs of frequency ratios should define the most robust tori in three DOF. Fig. 4a shows a plot of the spiral noble pairs of frequency ratios in the region of the frequency ratio plane corresponding to the dynamically accessible range for planar OCS at 20000 cm^{-1}, as determined by the algorithm of Kim and Ostlund [23] ($\approx$450000 points are plotted). It is observed that these points, corresponding to robust tori, avoid the low-order resonance lines.

A picture of transport and trapping suggests itself, based on diffusion through the "maze" of the robust tori. Regions where persistent tori are densely distributed trap the trajectory for long times, while the unblocked resonance zones allow rapid flow between resonance junctions. Bottlenecks along resonance lines (see below) may result from a "pinching" of the resonance zone by families of robust tori (cf. the 3 : 2 resonance zone shown in fig. 4b).

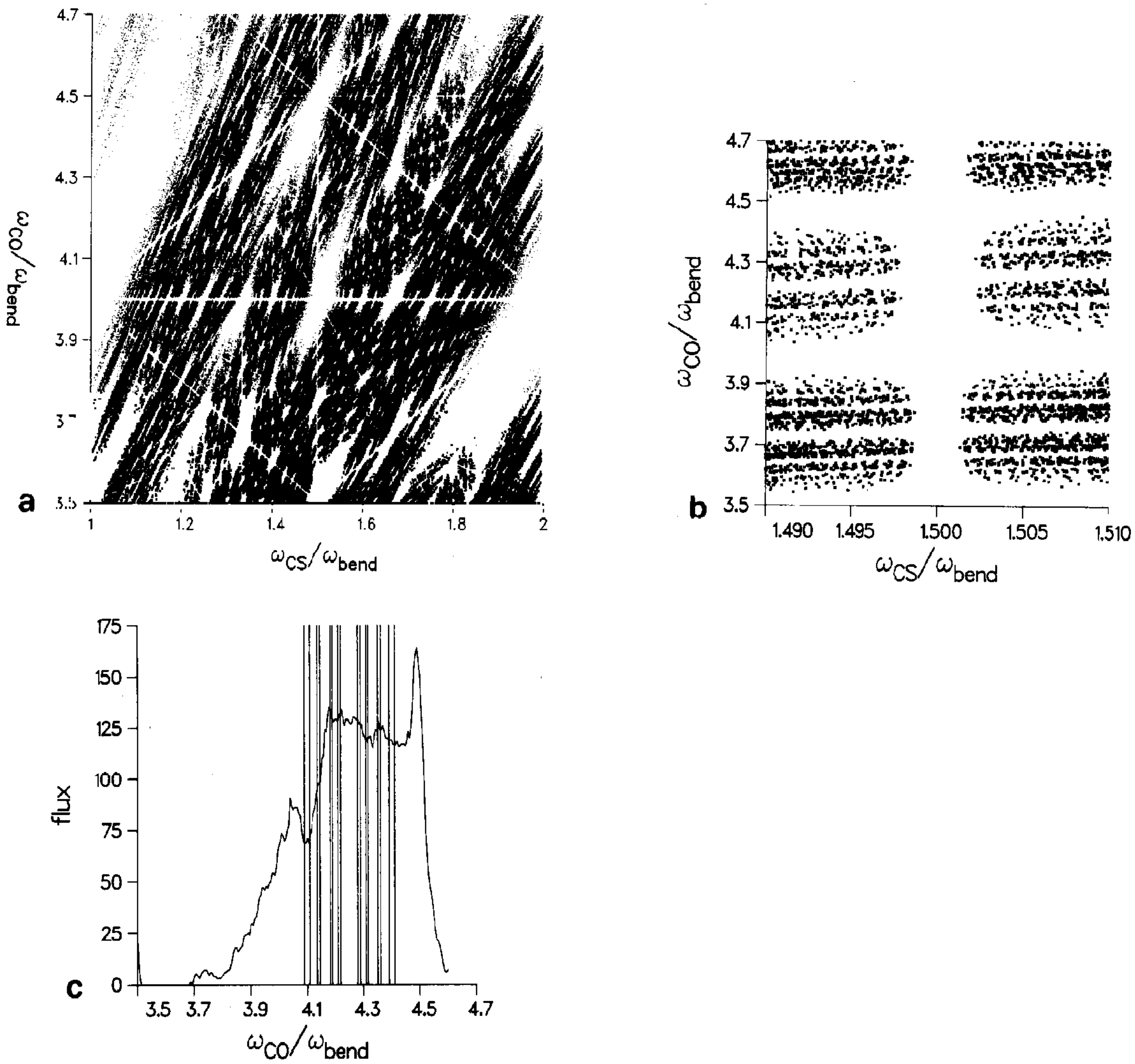

Fig. 4. (a) A subset of the 2^{22} most irrational pairs derived from the algorithm of Kim and Ostlund [23]. There are ≈450000 points in the range shown in the figure, which is appropriate for OCS. (b) Expanded view of part of (a) near the 3 : 2 resonance line. (c) This plot shows the number of crossings of frequency ratio surfaces near the 3 : 2 resonance line. The surfaces are defined by $\omega_{CO}/\omega_{bend}$ = constant, $\omega_{CS}/\omega_{bend} = 1.5 \pm 0.01$. The number of crossings observed for sequential segments of 400 trajectories is plotted versus $\omega_{CO}/\omega_{bend}$. The vertical lines correspond to the values of the ω_{O}/ω_{bend} ratio associated with the 16 most irrational pairs of frequency ratios, with one pair constrained to be 3 : 2. These were derived using the Kim and Ostlund algorithm [23], and are related to the "pinching" observed in (b).

In the second approach, the dynamics is taken to consist of a sequence of transitions between neighborhoods of resonance junctions, as seen in the first 20 ps of the trajectory in fig. 3. Transport is expected to occur along resonance lines joining the junctions. The fundamental question is then: "Are there barriers to transport along resonance lines, i.e. bottlenecks to Arnold diffusion?". We are investigating the possibility that bottlenecks along resonance zones can be defined by an irrationality condition involving in general all three frequencies of the motion, subject to a single resonance constraint $\boldsymbol{k}_{res} \cdot \boldsymbol{\omega} = 0$, where $\boldsymbol{k}_{res}$ defines the resonance zone connecting the initial and final junctions [15]. It is possible to systematically generate appropriate pairs of frequency ratios via the spiral noble construction of Kim and Ostlund [23]. Local frequency analysis can be used to calculate the flux along a resonance zone between a pair of resonance junctions through a surface defined by an independent frequency ratio, and a comparison made with the spiral noble results. This is done in fig. 4c, which shows the flux along the (3, −2, 0) resonance line as a function of the CO/CS frequency ratio. It is suggestive that one of the most pronounced minima in the flux (at $\omega_{CO}/\omega_{CS} \approx 4.1$) occurs in the vicinity of 2 of the 16 most irrational frequency ratios; this point is currently under study [15].

By identifying points of minimum flux lying along the dense set of resonance lines emanating from a given junction, it may be possible to construct a 4D partial barrier enclosing the junction. It is not clear whether the resulting surface in frequency ratio space would be smooth and differentiable or fractal.

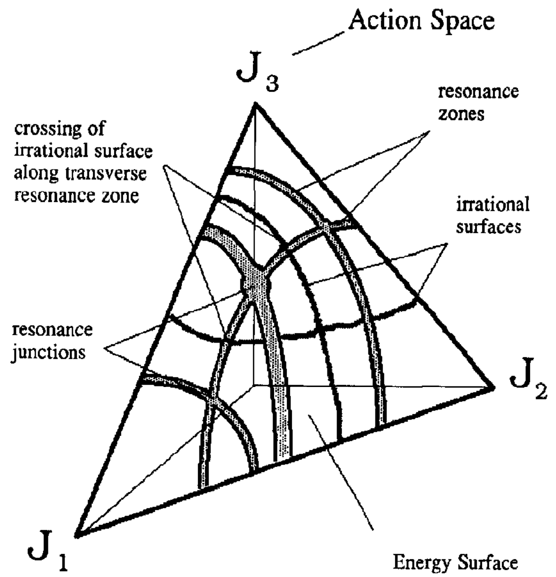

Fig. 5. Schematic view of phase space structure for three-degree of freedom systems, such as planar OCS.

5. Conclusion

The ideas and results on IVR in multimode systems presented here raise many interesting and unresolved questions. Local frequency analysis of chaotic trajectories for planar OCS suggests certain plausible mechanisms for transport and trapping in three-DOF systems, and the resulting view of the phase space structure in three DOF is shown schematically in fig. 5. The Hamiltonian used for planar OCS is very complicated, however, and trajectory integration takes a large amount of computer time. Planar OCS is also strongly chaotic at the energy studied. Study of simpler, more weakly coupled model systems is clearly needed to test our ideas more fully. Preliminary results [15] on transport in coupled standard maps [22] lend support to the picture developed here.

Our work establishes the utility of local frequency analysis as a method for studying chaotic dynamics of multimode systems, and application to other problems of chemical interest should yield interesting results. The quantum manifestations [24] of classical barriers in $N \geqslant 3$ DOF is an open question.

Acknowledgement

We are pleased to acknowledge stimulating discussions with Richard E. Gillilan and William P. Reinhardt. The work carried out at Cornell University was supported by NSF Grant CHE-8410685. The work at Argonne National Laboratory was supported by the Office of Basic Energy Sciences, Division of Chemical Sciences, US Department of Energy, under contract No. W-31-109-ENG-38. CCM wishes to thank the Department of Educational Programmes at Argonne National Laboratory for making his visit possible, and the members of the Theoretical Chemistry Group for their hospitality during his stay. CCM acknowledges support of the US Army Research Office, through the Mathematical Sciences Institute of Cornell University.

References

[1] M.J. Davis, J. Chem. Phys. 83 (1985) 1016.
[2] M.J. Davis and S.K. Gray, J. Chem. Phys. 84 (1986) 5389; S.K. Gray, S.A. Rice and M.J. Davis, J. Phys. Chem. 90 (1986) 3470.
[3] S.K. Gray and S.A. Rice, J. Chem. Phys. 86 (1987) 2020.
[4] M.J. Davis, J. Chem. Phys. 86 (1987) 3978.
[5] R.T. Skodje and M.J. Davis, to be published.

[6] R.S. MacKay, J.D. Meiss and I.C. Percival, Physica 13D (1984) 55.
[7] D. Bensimon and L.P. Kadanoff, Physica 13D (1984) 82.
[8] S.R. Channon and J. Lebowitz, Ann. NY Acad. Sci. 357 (1980) 108.
[9] R.S. MacKay, J.D. Meiss and I.C. Percival, Physica 27D (1987) 1.
[10] J.D. Meiss and E. Ott, Physica 20D (1986) 387.
[11] A.J. Lichtenberg and M.A. Lieberman, Regular and stochastic motion (Springer, Berlin, 1983).
[12] C.C. Martens and G.S. Ezra, J. Chem. Phys. 86 (1987) 279.
[13] D. Carter and P. Brumer, J. Chem. Phys. 77 (1982) 4208.
[14] M.J. Davis and A.F. Wagner, in: Resonances in electron–molecule scattering, van der Waals complexes, and reactive chemical dynamics, ed. D.G. Truhlar, Am. Chem. Soc. Symp. Ser. (1984).
[15] C.C. Martens, M.J. Davis and G.S. Ezra, in preparation.
[16] R.E. Gillilan and W.P. Reinhardt, Chem. Phys. Letters, to be published.
[17] R.D. Ruth, Lecture Notes Phys. 247 (1986) 37.
[18] Ya.G. Sinai, Acta Phys. Austr. Suppl. 10 (1973) 575.
[19] I. Hamilton and P. Brumer, J. Chem. Phys. 78 (1983) 2682.
[20] J.D. McDonald and R.A. Marcus, J. Chem. Phys. 65 (1976) 2180.
[21] R.A. Marcus, W.L. Hase and K.N. Swamy, J. Phys. Chem. 88 (1984) 6717.
[22] K. Kaneko and R.J. Bagley, Phys. Letters A110 (1985) 435.
[23] S.H. Kim and S. Ostlund, Phys. Rev. A34 (1986) 3426.
[24] G. Radons, T. Geisel and J. Rubner, Advan. Chem. Phys., to be published.